SAND2023-00571C

ARMA 23-512

Benchtop Experimental Studies of Stick-slip Mitigation Methods

Hilborn, H.
School of Mechanical Engineering, Georgia Institute of Technology, Atlanta, GA, United States
Jorgenson, H.
University of South Florida, Tampa, FL, United States
Su, J.-C.
Sandia National Laboratories, Albuquerque, NM, United States
Mazumdar, A.
School of Mechanical Engineering, Georgia Institute of Technology, Atlanta, GA, United States

ABSTRACT: Drilling vibrations can cause inefficient drilling and accelerated damage to system components. Therefore, reducing or eliminating such vibrations is a major focus area for natural gas and geothermal drilling applications. One particularly important vibration mode is stick-slip. Stick-slip occurs when the bottom-hole angular velocity starts oscillating while the top hole angular velocity remains relatively constant. This not only causes poor drilling, it is also difficult to detect using surface sensors. In this work, we describe the development and testing of a benchtop drilling system for studying stick-slip dynamics and mitigation. We show how this system can produce stick-slip oscillations. Next, we use this data to formulate a data-driven rock-bit interaction model. This model can be combined with linear systems analysis to predict stick-slip and understand mitigation methods. We describe out instrumentation that enables closed-loop control under simulated communications constraints. We conclude by providing preliminary experimental data on bench-level stick-slip.

1 INTRODUCTION

Exploration via autonomous drilling processes for geothermal resources is an important focus area for drilling research. However, to fully realize the clean-energy promise of geothermal energy, key challenges still need to be resolved.

Issues arising in the drilling process often originate from a drill-string's increased susceptibility to vibrational oscillations as depths increase. Some examples of drilling vibrations include stick-slip (Navarro-Lopez and Suarez (2004)), bit-bounce (Spanos et al. (1995)), and whirl (Jansen (1991)). Torsional oscillations are the focus of this work.

Torsional vibrations result in a destructive phenomenon known as stick-slip. Initiated at the bit-rock surface, the drill-string bit experiences large angular velocity oscillations not seen at the surface (Pavone and Desplans (1994); Besselink et al. (2011); Kessai et al. (2020)). Stick-slip results in premature bit wear and drill-string fracture.

Stick-slip is a fundamentally nonlinear and unpredictable phenomena. Stick-slip results from the combination of bit-rock interactions and drill-string compliance. As a result, there is a key need for experimental studies of stick-slip dynamics and mitigation.

This work presents a scaled test-rig for experimental validation of stick-slip oscillation of a 2-DoF torsional system. This investigation contributes the following (1) the description of a benchtop experimental setup for evaluating stick-slip, (2) a data-driven rock-bit model that predicts stick-slip behavior, and (3) preliminary experimental results using closed-loop control with delayed bit infor-

Sandia National Laboratories is a multimission laboratory managed and operated by National Technology & Engineering Solutions of Sandia, LLC, a wholly owned subsidiary of Honeywell International Inc., for the U.S. Department of Energy's National Nuclear Security Administration under contract DE-NA0003525.

mation.

This paper is structured as follows. Section 3 provides a description of the benchtop test-rig. Sections 4 and 5 detail an overview of model dynamics, control system design and benchtop physical parameters as related to full-scale drill-string parameters. Section 6 summarizes initial experimental results which highlight the presence of stick-slip behaviors.

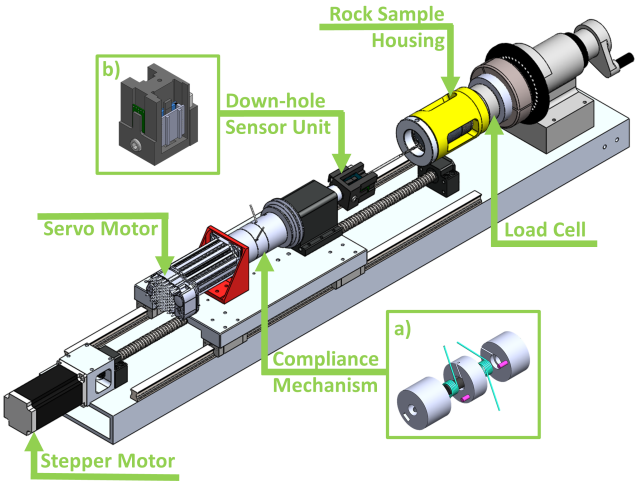

Fig. 1: Test Rig Overview.

2 BACKGROUND

2.1. Stick-Slip Oscillations

Authors have proposed many explanations for stick-slip. Liu et al. (2014) postulates the torsional mode being the dominant contributor causing drill-string damage and expediting failure. Tang and Zhu (2020) found torsional vibrations are inclined to appear in deep-drilling scenarios, a very cost intensive process. Hance (2005) estimates that up to 56 percent of the cost variability of geothermal well development is linked to depth. This necessitates the development of models to efficiently augment geothermal drilling progress.

Analysis of torsional drill-string vibrations highlights how stick-slip occurs only when in contact with rock, whereas absent when lacking contact (Brett (1992)). This emphasizes the importance of including a bit-rock interaction model in when modeling stick-slip performance.

Previous works have developed varying non-linear friction models for bit-rock interaction contribution. Static friction models can be derived from the classical Coulomb friction model (Lin and Wang (1991); Jansen and van den Steen (1995)). Navarro-Lopez and Suarez (2004) uses the velocity-weakening model, where a decrease in torque-on-bit (TOB) corresponds to increasing bit angular velocity with constant weight-on-bit (WOB). Alternatively, Richard et al. (2004) utilizes drag bit features, where the bit-rock interaction can be decomposed into cutting and frictional forces. Ultimately, the cutting frictional net effect displays the important velocity weakening effect (Kamel and Yigit (2014)).

Early experimental research pioneered field studies facilitating data collection at the top of the drill-string. Finnie and Bailey (1960) observed coupling between longitudinal and torsional vibration, but there was no ability to observe down-hole conditions. Pavone and Desplans (1994) performed further field experimentation, observing the stick-slip phenomenon with development of a down-hole measurement unit. This important work provided valuable data on stick-slip dynamics and mitigation methods. We leverage this past work in this paper.

Recent experimentation by Zhang et al. (2020) utilized a measurement tool to study down-hole behavior in a ultra-deep well, where severe stick oscillations were generated. Field experimentation often utilizes existing drill sites, offers the greatest accuracy, but incurs high costs.

2.2. Laboratory Examination of Stick-Slip

Laboratory experimental analysis offers an intermediate solution, enabling rapid model validation and cost-effective experimentation. Brett (1992) demonstrated good correlation between laboratory and field experimentation. This shows laboratory experimental systems have the potential to provide further insight into drill-string dynamic behavior. Laboratory tests can be performed frequently, under controlled conditions, and can utilize prototype hardware components.

Laboratory drilling systems commonly use a motor to command top hole angular velocity. Real et al. (2018); Kovalyshen (2014) display laboratory experiments implementing rock samples for drilling. Alternatively, Abdo et al. (2019); Khulief and Al-Sulaiman (2009) utilize braking mechanisms and shaker plates in respective laboratory systems, stimulating drill-string vibrations in the absence of rock and drilling mechanisms. Sharma et al. (2020) presents an open-loop laboratory experimental setup, exploring crucial factors such as sensor quality and down-hole sampling rate, resulting in the successful identification of stick-slip oscillations. Wiercigroch et al. (2017); Real et al. (2018); Mihajlović et al. (2004) laboratory setups utilize a slender rod to represent the drill-string in a minimized degree-of-freedom(DoF) setup. Large scale laboratory setups (Xu et al. (2021); Elsayed and Aissi (2006)) are capable of producing WOB loads closer to

field conditions, but require a large spatial footprint.

2.3. Stick-slip Mitigation using Feedback Control

Many methods for controlling unwanted drill-string vibrations have been pursued. Passive control solutions to vibration control involve design and optimization of down-hole instrumentation or vibration absorbing tools implemented down-hole (Zhu et al. (2014); Viguié et al.). Active control methods vary system inputs like weight-on-bit and rotational rate to influence drilling behavior. These have been frequently utilized to stabilize drilling vibrations (Brett (1992); Halsey et al. (1988); Serrarens et al. (1998); Yigit and Christoforou (2000); Christoforou and Yigit (2003)). It has been observed that increasing bit velocity or decreasing WOB (Jansen and van den Steen (1995); Pavone and Desplans (1994)) can aid in decreasing stick-slip oscillations. However, due to the nonlinear friction relationship seen at the bit-rock surface, controller designs must be able to handle changing parameters resulting from bit-rock nonlinearities. Losoya et al. (2018) implements control techniques for stick-slip stabilization in a laboratory experimental test-rig.

2.4. Communication Challenges

A key challenge in using closed-loop control is associated with communicating down-hole information to the surface control system. An exciting method for high-speed communication involves wired-telemetry. This enables high-speed, continuous data transmission. However, wired methods can fail due to drilling abrasions sustained in the drilling process, also incurring substantial installation and maintenance costs (Cheng and Tianhuai (2010)).

Drilling systems can use wireless telemetry methods for drill-string measurement-while-drilling (MWD) schemes. Common wireless methods include mud-pulse telemetry, extremely low frequency electromagnetic (EM) telemetry, and acoustic telemetry. Commercially available technologies utilize mud-pulse telemetry, but this method suffers from some important constraints. Mud pulse telemetry uses mud pressure signal pulses that travel along the drilling pipe to deliver data to the surface, but at low transmission speeds (Jaeger (2014)). Additionally, mud-pulse suffers from relatively low data transmission rates (approx. 10-40 bits/s) (Berro and Reich (2019)). Thus, transmission characteristics make mud-pulse telemetry difficult to utilize in control schemes. EM telemetry also has challenges. EM telemetry can encounter undesirable high attenuation in specific drilling circumstances (Sch (2009)).

Acoustic telemetry offers promise for our stick-slip measurement and control. Acoustic telemetry offers theoretical transmission speeds 1-2 orders of magnitude over EM and mud-pulse telemetry (Xie et al. (2021)). Field test programs evaluated acoustic telemetry, meriting good performance for commercial application (Nef (2007)). Deep drilled wells may exhibit banded transmission characteristics and surface signal degradation (Sinanovic et al. (2004)) due to the periodic nature of the drill-string structure. In these cases, signal rectification occurs via installation of repeater systems. However, Shin (2021) shows promising QPSK-modulation. This enables fast and accurate data transmission, without the need for signal repeaters. Thus, the increased signal data transmission rate and increased signal reliability of acoustic telemetry is favorable for control design schemes.

3 EXPERIMENTAL SYSTEM OVERVIEW

This section describes a bench-level system for studying drilling stick-slip behaviors.

3.1. Physical System Description

An overview of the benchtop experimental system can be seen in Figure 1.The test-rig is comprised of (i) axial motion assembly, (ii) torsional motion assembly, and (iii) down-hole sensing assembly. The axial motion assembly consists of a stepper motor to drive linear motion via a lead screw. The torsional motion assembly consists of a servo-motor simulating table-surface rotational motion. A 2-DoF drill-string is represented by a 3D printed mass-spring device, providing decreased system rigidity. Viewable in Figure 1a, torsion springs are placed in series within a housing mechanism that limits angle displacement to the spring maximum of 120 degrees. This elastic component can be tailored depending on the desired dynamics, and enables study of compliant drilling systems. The drill-string compliance mechanism translates motion down the drill-string via attachment to a lathe headstock, which holds a 1/8 inch carbide drill bit. Drilling occurs into 3 inch diameter rock samples (in this work, Mancos Shale), located in a custom core sample housing. The rock sample housing is placed in a rotating collet holder.

3.2. System Sensing

Displacement data acquisition is collected via a linear encoder attached to the drill-string frame. Down-hole data acquisition is simulated via a sensing unit (Fig. 1b) attached to the drill bit. This sensor module enables collection of angular velocity data as drilling occurs. The sensor module houses a gyroscope, an Arduino Pro Mini microcontoller, a Xbee antenna module and a battery. The antenna module provides wireless data transmission back to the main computer for data collection. All elements housed are designed for equal mass distribution. Top-hole angular velocity is collected from the servo-motor via a digital output, which is used to measure motor speed.

Lastly, a load cell is attached to the rock core sample housing to obtain force and torque values. This load cell is used to measure the bit-rock interaction forces and moments. A visual overview of these processes can be viewed in Figure 2. All instrumentation signaling and data acquisition is performed through a customized Labview interface. This system was originally developed at Sandia National Laboratories and has been refined through collaboration with Georgia Tech.

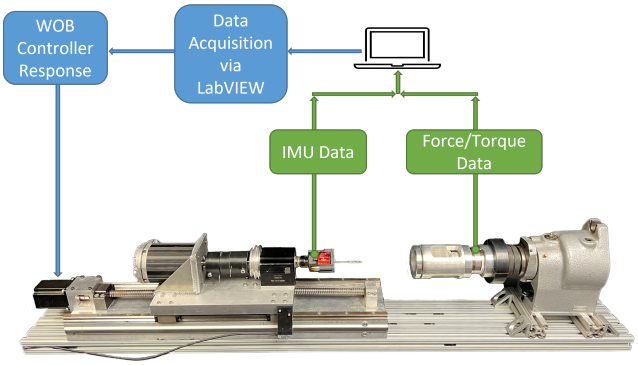

Fig. 2: Data Acquisition Process.

3.3. Control Modes

Two control modes are available for this benchtop experimental setup. Open-loop control occurs at a set feed rate, with no axial force feedback. Alternatively, WOB control mode occurs with inclusion of load cell force feedback. Both control modes command a constant top-hole angular velocity. Utilizing both modes, we are able to easily perform controller prototyping via the following workflow. The benchtop test-rig is easily modified to collect data for a desired bit and rock combination. The experimental setup can also be quickly switched between rigid and compliant mode.

4 LINEARIZED DRILL-STRING DYNAMIC MODEL

Linearized analysis is a common method for examining dynamics and control. This study utilizes a lumped parameter representation of a 2-DoF mechanical system, depicted in Figure 3. Such 2-DoF lumped parameter models have been used in past studies of stick-slip (Kapitaniak et al. (2015); Jansen and van den Steen (1995)).

4.1. Mechanical System Dynamics

We approximate the surface drive for a drill as a speed-controlled motor. We assume that the top-hole speed is reasonably well regulated. This could be done using a closed-loop controller that regulates the top hole speed (ω_1) automatically. The top-hole speed can also be held

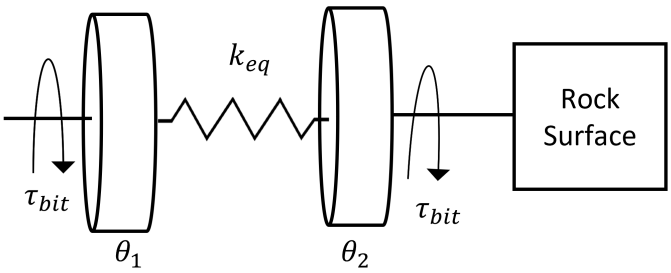

Fig. 3: 2-DoF Torsional Drill-string Model.

reasonably constant using open-loop speed control. In the case of this work, we use a stepper motor commanded with a constant frequency pulse train. This is an open-loop control strategy, but we found that the top-hole speed remains relatively constant during our experiments.

The key dynamics are therefore associated with the torsional spring and the motion of the bit. Many approximations for drill-strings use a 2-inertia lumped parameter model. They are computationally simpler and easier to integrate into linear control system analysis.

In this work, we use the same type of approximation. However, in this case, this approximation is almost identical to our physical system. This is because we use a single torsional spring to emulate the drill string compliance.

The 2-DoF model can be defined by the following set of dynamic equations:

$$\dot{\theta}_1 = \omega_1 \tag{1}$$

$$\dot{\omega}_1 = 0 \tag{2}$$

$$J_2\ddot{\theta}_2 + k_{eq}(\theta_2 - \theta_1) + c_2(\dot{\theta}_2 - \dot{\theta}_1) + \tau_b = 0 \tag{3}$$

τ_b denotes the rock-bit friction torque at the drilling surface.

4.2. Rock-bit Interaction Dynamics

In this work we assume a rock-bit interaction model that is loosely based on that of Pavone and Desplans (1994). Specifically, this model assumes that the bit torque, τ_b is related to the weight on bit (WOB) raised to a power and the bit speed (ω_2) raised to a b.

$$\tau_b = \mu \cdot F_2^a \cdot \dot{\theta}_2^b \tag{4}$$

where F_2 represents down-hole weight-on-bit, and $\dot{\theta}_2$ represents down-hole angular velocity.

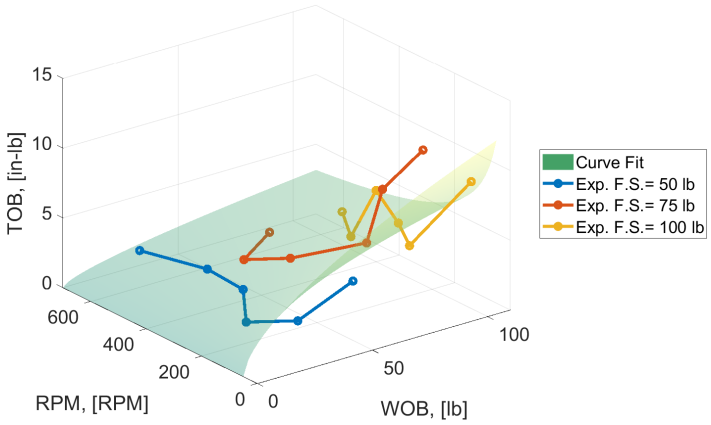

Fig. 4: Experimental Velocity Weakening Effect

We perform an initial experimental sweep by varying open-loop feed control input. Bit-rock data collection occurs with a rigid coupling. Respective data analysis will output three parameters: μ, a, and b. These parameters create the bit-rock model (See Eq. 5). Using desired field drillstring dynamics and collected bit-rock model data, parameters are then transferred to simulated space, where we can analyze the frequency response of the system. Within the frequency domain, we can rapidly develop optimal controller parameters.

An initial experimentation sweep was performed with the experimental test-rig to validate the velocity weakening frictional model referenced. These data were collected with the benchtop drillstring represented with a rigid coupling. The following bit-rock model coefficients were extracted ($\mu = 0.07$, $a = 0.6$, $b =$ -0.49) via MATLAB curvefit toolbox, utilizing experimental data plotted in Figure 4.
To take near zero and negative speeds into account, bit-rock contact smoothing was included Pavone and Desplans (1994). The inclusion of this continuity can be represented by Equation 5.

$$\tau_{b,s} = \tau_b \cdot (1 - e^{\frac{RPM}{RPM_0}}) \tag{5}$$

The coefficient RPM_0 is obtained via numerical simulation. Varying values of RPM_0 are evaluated for a best match to data. A linearized version of the fitted bit-rock friction model is utilized for controller design. Although this does not fully capture the nonlinearities of the original friction model, it captures a sufficient approximation around chosen WOB and angular velocity values. The linearization can be approximated as the following:

$$\tau_b \approx \tau_{b,0} + a_1 \Delta F_2 + a_2 \Delta\dot{\theta}_2 \tag{6}$$

$$a_1 = a\gamma\omega_{2,0}^{b} F_{2,0}^{a-1} \tag{7}$$

$$a_2 = b\gamma F_{2,0}^{a} \omega_{2,0}^{b-1} \tag{8}$$

where $a = 0.6$ and $b =$ -0.49. ΔF_2 and $\Delta\dot{\theta}_2$ are operational conditions which our system is linearized about. Using frequency domain analysis tools, in tandem with our linearized rock bit interaction model, we can generate our system plant model as the following:

$$G_p(s) = \frac{\Delta\dot{\theta}_2(s)}{\Delta F_2(s)} = \frac{-a_1 s}{J_2 s^2 + a_2 s + B_2 s + K_c} \tag{9}$$

The system output is down-hole angular velocity, and the input is surface table force. Under open loop conditions, the plant poles will always lie in the right-hand side of the imaginary axis, representing inherent system instability.

4.3. Communication Dynamics

Feedback control requires sensor feedback. As we have described previously, stick-slip oscillations are not readily measured using surface rotational speed sensors. This means that other sensors must be used for stick-slip control. Down-hole sensors can provide valuable information for closed-loop control. However, down-hole information must be transmitted to the surface before it can be used for control.

In this work, we examine acoustic telemetry in greater detail. This acoustic telemetry communication method transmits data utilizing pressure wave propagation. As shown in Mwachaka et al. (2019), due to lower attenuation at greater depths, low data rates with simple modulation schemes are commonly used. Acoustic telemetry methods often suffer from added noise; this model neglects noise, and assumes two 8-bit numbers are needed from the down-hole sensing system ($\dot{\theta}_2$, $\ddot{\theta}_2$).

We can simplify communication dynamics with the following model assumptions.

The first element of wireless communication is low data rates. These can be modeled as a zero-order-hold (ZOH), assumed to be held at a fixed period T.

$$G_{ZOH}(s) = \frac{1 - e^{-Ts}}{Ts} \tag{10}$$

The second element of wireless communication is pure transmission delay. This is produced from the phenomenon of speed of sound traveling through surrounding terrain, a term associated with the length of the drill-string. This is shown in Eq. 11).

$$G_{delay}(s) = e^{-t_{delay}s} \tag{11}$$

A pure time delay, however, cannot be represented with a transfer function notation. We approximate with 2^{nd} order Pade' approximation (Eq. 12), used to provide greater

approximation accuracy.

$$e^{-as} \approx \frac{a^2s^2 - 6as + 12}{a^2s^2 + 6as + 12} \tag{12}$$

This can be used to create transfer functions for both the ZOH and the pure delay.

$$G_s(s) = \frac{\omega_{2,meas}(s)}{\omega_1(s)} = G_{ZOH}(s)G_{delay}(s) \tag{13}$$

where

$$G_{ZOH}(s) \approx \frac{12}{T^2s^2 + 6Ts + 12} \tag{14}$$

$$G_{delay}(s) \approx \frac{t_{delay}^2 s^2 - 6t_{delay}s + 12}{t_{delay}^2 s^2 + 6t_{delay}s + 12} \tag{15}$$

4.4. Axial Force Dynamics

The last challenge is associated with force transmission from the surface to the bit. We assume that force also travels as a pressure wave down the drill-string back to the bit. This again incurs a pure transmission delay. This delay is associated with the speed of sound in the drill-string. This means that there are two pure delays in the loop transmission of the control loop. In this case (acoustic telemetry), the two delays can be approximated as roughly equal in nature. Axial force transmission dynamics are represented by the transfer function $G_a(s)$.

The overall loop transmission function can be modeled as follows.

$$G_{loop}(s) = K_p(s)G_p(s)G_s(s)G_a(s) \tag{16}$$

For the following simulations, the corresponding simulated versus physical system parameters can seen in Table 1. Values for t_{delay} roughly correspond to a physical drill-string of 3000 meters in depth.

Table 1: Drill-string Model Parameters.

Parameter	Simulated	Experimental
k_{th} (Nm·rad^{-1})	386.6	0.1772
ω_n [Hz]	1.480	0.7074
J_2 (kg·m^2)	617.6	0.7083
t_{delay}	0.5172	0.5172
T	0.25	0.25

5 CONTROL DESIGN AND STABILITY ANALYSIS

5.1. Control Architecture

Active feedback control can help augment drill-string stability. By using feedback of system-states, the closed loop

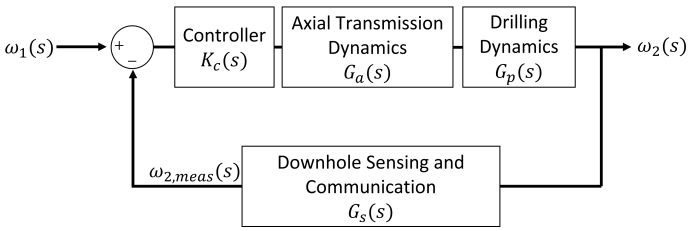

Fig. 5: System Block Diagram.

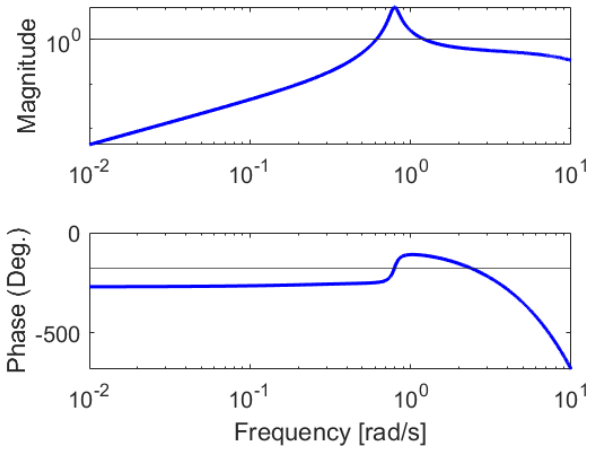

Fig. 6: Benchtop Parameters, Frequency Response

poles can be moved to the stable region of the complex plane. One method utilized is using the surface force to increase WOB in response to differences between the top and bottom hole rotation rates Pavone and Desplans (1994); Navarro-Lopez and Suarez (2004).

A controller of the following architecture is used.

$$\Delta F_1(s) = K_c(s)(\omega_1(s) - \omega_{2,meas}(s)) \tag{17}$$

This structure is illustrated in the block diagram shown in Fig. 5. The loop transmission transfer function, G_{loop} with tuned feedback gain is shown in Fig. 6.

$$G_{CL}(s) = \frac{K_c(s)G_p(s)}{1 + K_c(s)G_p(s)G_s(s)} \tag{18}$$

$$K_c(s) = K(s + z_c) \tag{19}$$

Frequency-domain analysis is utilized for controller design. The benchtop system loop transfer function is comprised only of the plant, controller, and zero-order-hold. Software delays can be added to emulate down hole wireless telemetry and axial dynamics. Frequency domain analysis is used to manipulate loop gain, K, for desired phase characteristics that maintain closed-loop stability.

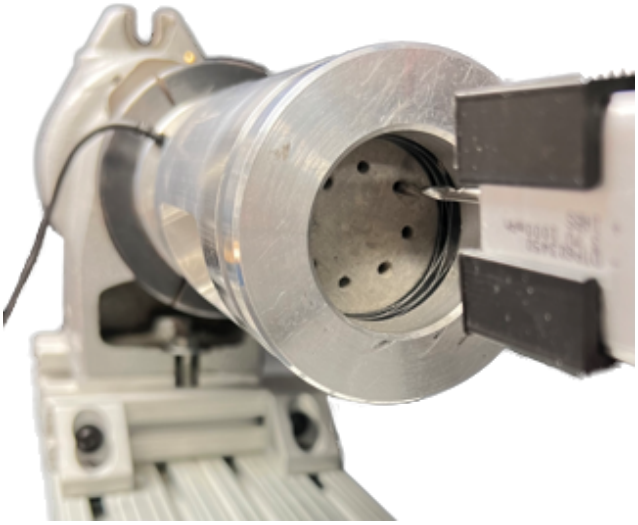

Fig. 7: Laboratory Bit-Rock Drilling Interface.

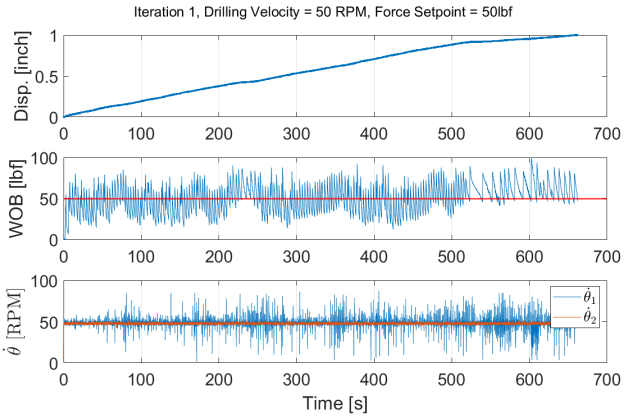

Fig. 8: Experimental Result:WOB Control, stick-slip present.

6 EXPERIMENTAL RESULTS

Benchtop drilling experiments utilized Mancos Shale rock core specimen. Commanded surface angular velocities range from 50 to 600 RPM. Drilled shale cores are 3 inches in length, 1.5 inches in diameter, providing up to 12 experiments per specimen. Figure 7 displays the 8th rock specimen experimental run as drilling begins, from a down-hole drilling point-of-view.

6.1. Experimental Torsional Vibrations

Primary drilling experimentation was performed with WOB control but not down hole velocity feedback. Future work can utilize the down hole feedback we described in the previous section. One example experiment is shown in Fig. 8. This data illustrates how our test bed is able to replicate stick-slip drilling behavior.

These experimental results represent initial drillstring dynamics with lesser drillstring inertia than represented in Table 1. The experimental system inertia for these data is evaluated to be $0.011 kg \cdot m^2$. This only represents motor, bit and sensing unit inertia, and incompletely captures field drillstring parameters we hope to control. However, our drillstring device is easily modified. An alternative 3D-printed end-piece will account for attaching additional mass that can be modulated to emulate any field drillstring parameters given. Thus, with modifications, we achieve system dynamics shown in Fig. 6.

7 CONCLUSIONS

This work presents the design, analysis, and preliminary experimental results for a benchtop drilling system. This system is designed to study stick-slip oscillations. We have shown how the bench-level system can recreate stick-slip oscillations during rock drilling. This system provides a way to rapidly study stick-slip dynamics and evaluate control and sensing methods. We have also outlined our proposed feedback control architecture. Future work will focus on implementing the control archicture and examining the effect on stick-slip behavors.

ACKNOWLEDGMENTS

This project was supported by the DOE Office of Energy Efficiency and Renewable Energy. This paper describes objective technical results and analysis. Any subjective views or opinions that might be expressed in the paper do not necessarily represent the views of the U.S. Department of Energy or the United States Government. Sandia National Laboratories is a multimission laboratory managed and operated by National Technology & Engineering Solutions of Sandia, LLC, a wholly owned subsidiary of Honeywell International Inc., for the U.S. Department of Energy's National Nuclear Security Administration under contract DE-NA0003525.

REFERENCES

1. (2007). *Field-Test Results of an Acoustic MWD System*, volume All Days of *SPE/IADC Drilling Conference and Exhibition*. SPE-105021-MS.

2. (2009). *Signal Attenuation for Electromagnetic Telemetry Systems*, volume All Days of *SPE/IADC Drilling Conference and Exhibition*. SPE-118872-MS.

3. Abdo, J., Hassan, E. M., Boulbrachene, K., and Kwak, J. C. T. (2019). Drillstring Failure-Identification, Modeling, and Experimental Characterization. *ASCE-ASME J Risk and Uncert in Engrg Sys Part B Mech Engrg*, 5(2):021004.

4. Berro, M. J. and Reich, M. (2019). Laboratory investigations of a hybrid mud pulse telemetry (HMPT)-A new approach for speeding up the transmitting of MWD/LWD data in deep boreholes. *Journal of Petroleum Science and Engineering*, 183:106374.

5. Besselink, B., van de Wouw, N., and Nijmeijer, H. (2011). A Semi-Analytical Study of Stick-Slip Oscillations in Drilling Systems. *Journal of Computational and Nonlinear Dynamics*, 6(2):021006.

6. Brett, J. (1992). The genesis of torsional drillstring vibrations. *SPE Drilling Engineering*, 7(3):168 â 174.

7. Cheng, L. and Tianhuai, D. (2010). Signal wireless transmission behaviors along the drillstring using extensional stress waves. In *2010 IEEE International Conference on Intelligent Computing and Intelligent Systems*, volume 2, pages 541–545.

8. Christoforou, A. and Yigit, A. (2003). Fully coupled vibrations of actively controlled drillstrings. *Journal of Sound and Vibration*, 267(5):1029–1045.

9. Elsayed, M. A. and Aissi, C. (2006). Analysis of Shock Absorber Characteristics for Drillstrings. In *Volume 3: Dynamic Systems and Controls, Symposium on Design and Analysis of Advanced Structures, and Tribology*, pages 93–101, Torino, Italy. ASMEDC.

10. Finnie, I. and Bailey, J. J. (1960). An Experimental Study of Drill-String Vibration. *Journal of Engineering for Industry*, 82(2):129–135.

11. Halsey, G., Kyllingstad, A., and Kylling, A. (1988). Torque Feedback Used to Cure Slip-Stick Motion. volume All Days of *SPE Annual Technical Conference and Exhibition*. SPE-18049-MS.

12. Hance, C. N. (2005). Factors Affecting Costs of Geothermal Power Development.

13. Jaeger, F. (2014). Experimental study: Measurement of sonic speed of drilling muds under shear stress. Technical report, IBJ Technology, Markkleeberg, DE.

14. Jansen, J. (1991). Non-linear rotor dynamics as applied to oilwell drillstring vibrations. *Journal of Sound and Vibration*, 147(1):115–135.

15. Jansen, J. and van den Steen, L. (1995). Active damping of self-excited torsional vibrations in oil well drillstrings. *Journal of Sound and Vibration*, 179(4):647–668.

16. Kamel, J. M. and Yigit, A. S. (2014). Modeling and analysis of stick-slip and bit bounce in oil well drillstrings equipped with drag bits. *Journal of Sound and Vibration*, 333(25):6885–6899.

17. Kapitaniak, M., Hamaneh, V. V., Chávez, J. P., Nandakumar, K., and Wiercigroch, M. (2015). Unveiling complexity of drill–string vibrations: Experiments and modelling. *International Journal of Mechanical Sciences*, 101:324–337.

18. Kessai, I., Benammar, S., Doghmane, M. Z., and Tee, K. F. (2020). Drill Bit Deformations in Rotary Drilling Systems under Large-Amplitude Stick-Slip Vibrations. *Applied Sciences*, 10(18):6523.

19. Khulief, Y. A. and Al-Sulaiman, F. A. (2009). Laboratory investigation of drillstring vibrations. *Proceedings of the Institution of Mechanical Engineers, Part C: Journal of Mechanical Engineering Science*, 223(10):2249–2262.

20. Kovalyshen, Y. (2014). Experiments on Stick-Slip Vibrations in Drilling with Drag Bits. volume All Days of *U.S. Rock Mechanics/Geomechanics Symposium*. ARMA-2014-7108.

21. Lin, Y.-Q. and Wang, Y.-H. (1991). Stick-Slip Vibration of Drill Strings. *Journal of Engineering for Industry*, 113(1):38–43.

22. Liu, X., Vlajic, N., Long, X., Meng, G., and Balachandran, B. (2014). State-Dependent Delay Influenced Drill-String Oscillations and Stability Analysis. *Journal of Vibration and Acoustics*, 136(5).

23. Losoya, E. Z., Gildin, E., and Noynaert, S. F. (2018). Real-time Rate of Penetration Optimization of an Autonomous Lab-Scale Rig using a Scheduled-Gain PID Controller and Mechanical Specific Energy. *IFAC-PapersOnLine*, 51(8):56–61.

24. Mihajlović, N., van Veggel, A. A., van de Wouw, N., and Nijmeijer, H. (2004). Analysis of Friction-Induced Limit Cycling in an Experimental Drill-String System. *Journal of Dynamic Systems, Measurement, and Control*, 126(4):709–720.

25. Mwachaka, S. M., Wu, A., and Fu, Q. (2019). A review of mud pulse telemetry signal impairments modeling and suppression methods. *Journal of Petroleum Exploration and Production Technology*, 9(1):779–792.

26. Navarro-Lopez, E. and Suarez, R. (2004). Practical approach to modelling and controlling stick-slip oscillations in oilwell drillstrings. In *Proceedings of the 2004 IEEE International Conference on Control Applications, 2004.*, volume 2, pages 1454–1460, Taipei, Taiwan. IEEE.

27. Pavone, D. and Desplans, J. (1994). Application of High Sampling Rate Downhole Measurements for Analysis and Cure of Stick-Slip in Drilling. All Days. SPE-28324-MS.

28. Real, F., Lobo, D., Ritto, T., and Pinto, F. (2018). Experimental analysis of stick-slip in drilling dynamics in a laboratory test-rig. *Journal of Petroleum Science and Engineering*, 170:755–762.

29. Richard, T., Germay, C., and Detournay, E. (2004). Self-excited stickâslip oscillations of drill bits. *Comptes Rendus MÃ©canique*, 332(8):619–626.

30. Serrarens, A., Van De Molengraft, M., Kok, J., and Van Den Steen, L. (1998). Hâ control for suppressing stick-slip in oil well drillstrings. *IEEE Control Systems*, 18(2):19 â 30.

31. Sharma, A., Srivastava, S., and Teodoriu, C. (2020). Experimental design, instrumentation, and testing of a laboratory-scale test rig for torsional vibrationsâthe next generation. *Energies*, 13(18).

32. Shin, Y. (2021). Simulation of QPSK-based acoustic telemetry through drillstring. *Journal of Mechanical Science and Technology*, 35(3):963–971.

33. Sinanovic, S., Johnson, D., Shah, V., and Gardner, W. (2004). Data communication along the drill string using acoustic waves. volume 4, pages iv – 909.

34. Spanos, P. D., Sengupta, A. K., Cunningham, R. A., and Paslay, P. R. (1995). Modeling of Roller Cone Bit Lift-Off Dynamics in Rotary Drilling. *Journal of Energy Resources Technology*, 117(3):197–207.

35. Tang, L. and Zhu, X. (2020). Effects of Drill String Length on Stick-Slip Oscillation of the Oilwell Drill String. *Iranian Journal of Science and Technology, Transactions of Mechanical Engineering*, 44(2):497–506.

36. Viguié, R., Kerschen, G., Golinval, J. C., McFarland, D. M., Bergman, L. A., Vakakis, A. F., and van de Wouw,

N. Using Targeted Energy Transfer to Stabilize Drill-string Systems. page 12.

37. Wiercigroch, M., Nandakumar, K., Pei, L., Kapitaniak, M., and Vaziri, V. (2017). State dependent delayed drill-string vibration: Theory, experiments and new model. *Procedia IUTAM*, 22:39–50. IUTAM Symposium on Nonlinear and Delayed Dynamics of Mechatronic Systems.

38. Xie, H., Zhang, P., and Zhou, J. (2021). Numerical study of drill string uncertainty in acoustic information transmission. *IOP Conference Series: Earth and Environmental Science*, 734(1):012024.

39. Xu, Y., Zhang, H., and Guan, Z. (2021). Dynamic Characteristics of Downhole Bit Load and Analysis of Conversion Efficiency of Drill String Vibration Energy. *Energies*, 14(1):229.

40. Yigit, A. and Christoforou, A. (2000). Coupled torsional and bending vibrations of actively controlled drillstrings. *Journal of Sound and Vibration*, 234(1):67–83.

41. Zhang, H., Di, Q., Li, N., Wang, W., and Chen, F. (2020). Measurement and simulation of nonlinear drillstring stick-âslip and whirling vibrations. *International Journal of Non-Linear Mechanics*, 125:103528.

42. Zhu, X., Tang, L., and Yang, Q. (2014). A Literature Review of Approaches for Stick-Slip Vibration Suppression in Oilwell Drillstring. *Advances in Mechanical Engineering*, 6:967952.